Hindawi
Journal of Nanomaterials
Volume 2022, Article ID 3979168, 12 pages
https://doi.org/10.1155/2022/3979168

Research Article

Heat and Mass Transfer of the Darcy-Forchheimer Casson Hybrid Nanofluid Flow due to an Extending Curved Surface

Gohar,[1] Tahir Saeed Khan,[1] Ndolane Sene,[2] Abir Mouldi,[3] and Ameni Brahmia[4]

[1]*Mathematics Department, University of Peshawar, Peshawar, Pakistan*
[2]*Laboratoire Lmdan, Departement De Mathematiques De Decision, Facultíe des Sciences Economiques et Gestion, Universite Cheikh Anta Diop De Dakar, BP 5683 Dakar Fann, Senegal*
[3]*Department of Industrial Engineering, College of Engineering, King Khalid University, Abha 61421, Saudi Arabia*
[4]*Chemistry Department, College of Science, King Khalid University, Abha 61413, Saudi Arabia*

Correspondence should be addressed to Ndolane Sene; ndolanesene@yahoo.fr

Received 11 October 2021; Revised 7 December 2021; Accepted 10 December 2021; Published 18 January 2022

Academic Editor: Amir Khan

The current paper describes a Darcy-Forchheimer flow of Casson hybrid nanofluid through an incessantly expanding curved surface. Darcy-Forchheimer influence expresses the viscous fluid flow in the porous medium. Carbon nanotubes (CNTs) with a cylindrical form and iron-oxide are utilized to make hybrid nanofluids. Using Karman's scaling, the principal equations are rearranged to nondimensional ordinary differential equations. The "Homotopy analysis method" is used to further build up the analytic arrangement of modeled equations. The impact of flow variables on the velocity and temperature profiles has been tabulated and explained. The flow velocity is raised when both the curvature and volume fraction parameters are elevated. The temperature and velocity profiles exhibit the opposite tendency when the Forchheimer number is increased, since the fluid velocity decreases while the energy profile grows. The addition of CNTs and iron nanocomposites improves the thermophysical characteristics of the base fluid significantly. The obtained consequences show that hybrid nanofluids are more efficient to improve the heat transfer rate. Using CNTs and nanomaterials in the base fluid to control the coolant level in industrial equipment is a wonderful idea.

1. Introduction

The flow over an extending surface has received much importance due to its significant role in several sectors of industry and engineering, such as condensation process, spinning of fiber and continuous casting of fiber, plastic sheet extraction, paper production, and many others. Crane [1] was the first to study the flow over an expanding planar surface. Many researchers have since followed the concept of the crane [2–5], expanding the sheets to investigate various aspects of this form of flow. Sajid et al. [6] addressed boundary layer flow and micropolar fluid, concluding that the curvature effect leads to a reduction in boundary layer size. Gul et al. [7] have investigated the flow of the boundary layer on the stretching surface using the Fractional Order Derivatives Scheme. Imtiaz et al. [8] demonstrated the fluid flow under the upshots of the magnetic field over an extending curved surface. It has been noticed that with the action of curvature coefficient, the energy profile is enhanced. Rosca et al. [9] have analyzed the flow caused by contracting and expanding sheets. Saeed et al. [10] offered a complete investigation of the Darcy hybrid nanoliquid flow through a curved surface that is exponentially expanding. The outcomes signify using SWCNTs, MWCNTs, and Fe3O4 nanomaterials for the increase in the nusselt number. Ali et al. [11] analyzed the hydrological importance of wave propagation of hybrid nanofluid over a warmed extended curved surface with the impacts of a magnetic field using bvp4c. The suspension of carbon nanotubes in a magnetite nanoliquid promotes local surface drag but reduces local heat flow. Kumar et al. [12]

have reported the radiation impact on the Casson fluid across the exponentially curved sheet. Hayat et al. [13] explored ferroliquid flow with the mass and heat transition across a curved stretching surface. Hussain et al. [14] reported the findings of their investigation on hybrid nanofluid flow across a curved sheet. The outcomes of the survey revealed that the energy transference efficiency in hybrid nanocrystals is higher than that in nanofluids for large frequencies of the curvature index. Qian et al. [15] and Khan evaluated that how heat transmission and radiation were affected by the conducting flow over a curved extending surface. Their study was found to be in good accord with a previously published finding.

The heat transmission in carbon nanofluids has gotten a lot of interest from researchers in a variety of fields in the last few years. CNTs are carbon nanotubes with a fundamental chemical structure and a carbon atom formation wrapped in a cylindrical shape. CNTs have superior chemical, thermophysical, and mechanical characteristics, making them ideal for usage as a particulate in a base fluid. They offer various advantages over other nanomaterials due to their tiny size, structure, configuration, dimension, and hardness. Haq et al. [16] evaluated the computational findings for conductive fluid using carbon nanomaterials along an extensive surface. Ahmadian et al. [17] addressed a 3D model of an unsustainable hybrid nanofluid flow with fluid and momentum transmission caused by surface accelerating displacement. The use of hybrid nanoparticles is thought to have enhanced the carrier fluid's thermal properties substantially. Because of the C–C link, CNTs are more effective than other forms of nanoparticles in the carrier fluid. CNTs nanofluid may be further functionalized to get the desired result, which may be used in a range of applications through noncovalent and covalent manipulation [18]. Saeed et al. [19] have considered the nanofluid containing CNTs and iron oxide nanomaterials using the flow of fluid over a curved surface. Gul et al. [20, 21] studied the flow of nanofluids to enhance heat transfer and thermal applications. Alghamdi et al. [22] have observed the flow of hybrid nanofluid through a blood artery for medications. Using the bvp4c tool, Li et al. [23], and Ding et al. [24] used (MWCNTs) in the base liquid to evaluate heat transmission. Akbar et al. [25] described the influence of a magnetic field on the flow of CNT nanofluids through a moving permeable channel. Gul et al. [26] and Bilal et al. [27] used an inclined extending cylinder to examine the Darcy-Forchhemier hybrid nanoliquid flow. They examined the carbon nanotubes (CNTs) and iron oxide Fe_3O_4 as two distinct nanomaterials. Ahmed et al. [28] represented temperature propagation in a wavy-wall impermeable enclosure through nanofluids. It was discovered that increasing the waviness of the sheet boosts both the heat transmission rate. Yarmand et al. [29] investigated how graphene nanoplatelets/platinum hybrid nanofluids with diverse properties may improve heat transfer rates. Sajid et al. [30] examined the thermophysical characteristics of hybrid and single-form nanotubes using numerical methods. They determined that the size, type, concentration, and temperature fluctuation of nanoparticles had a significant impact on the thermophysical characteristics of nanofluid. Kumar et al. [31] examined the solar radiation impact on the flow of ferromagnetic hybrid nanofluid. Gowda et al. [32] studied the flow of nanofluid over the stretched and curved surface using (KKL) relation. Kumar et al. [33] have used the concept of the magnetic dipole for the flow of nanofluid over a cylinder. Zeeshan et al. [34] have studied the couple stress nanofluid flow using the paraboloid model.

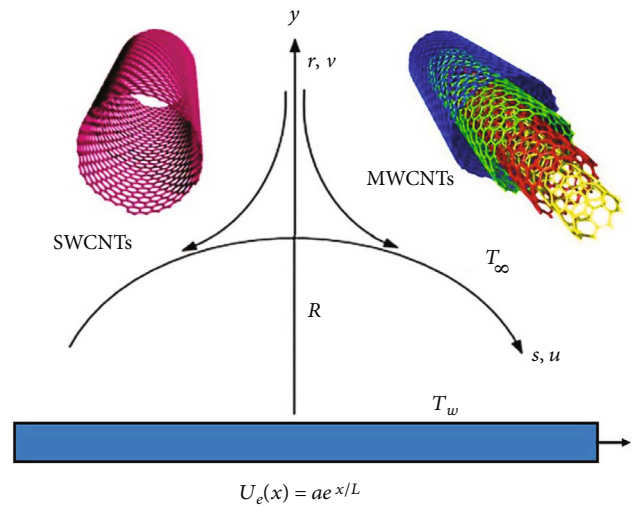

Figure 1: Physical sketch.

The curved surface for the fluid flow has many applications in the mechanical and automotive industry. Sanni et al. [35], Jawad et al. [36], and Saeed et al. [37] have studied the fluid flow on a curved surface using various kinds of nanofluids for the heat transfer enhancement. Hayat et al. [9, 38], Rosca, and Pop [39] have explained the homogeneous-heterogeneous reaction phenomena using the curved surface for the flow pattern. Okechi et al. [40], Asghar et al. [41], and Hayat et al. [42] have used the nonewtonian fluid flow over the curved surface with various extensions considering Darcy-Forchheimer flow medium. The related work to the proposed model can be seen in the References [9, 35, 43–45].

The inertia effect is taken into account by incorporating a squared component to the momentum equation, called Forchheimer's modification [46]. Muskat [47] used the term "Forchheimer factor" to describe this new concept. It is critical to include non-Darcy consequences in convective transport analysis to properly represent real-world challenges. The novelty of the model has been presented as

(i) For the hybrid nanofluid flow, heat and mass transmission is examined simultaneously

(ii) The $(\text{CNTs} + Fe_3O_4/H_2O)$ hybrid nanoliquid flow across a stretching surface with the mass and heat transition has been addressed

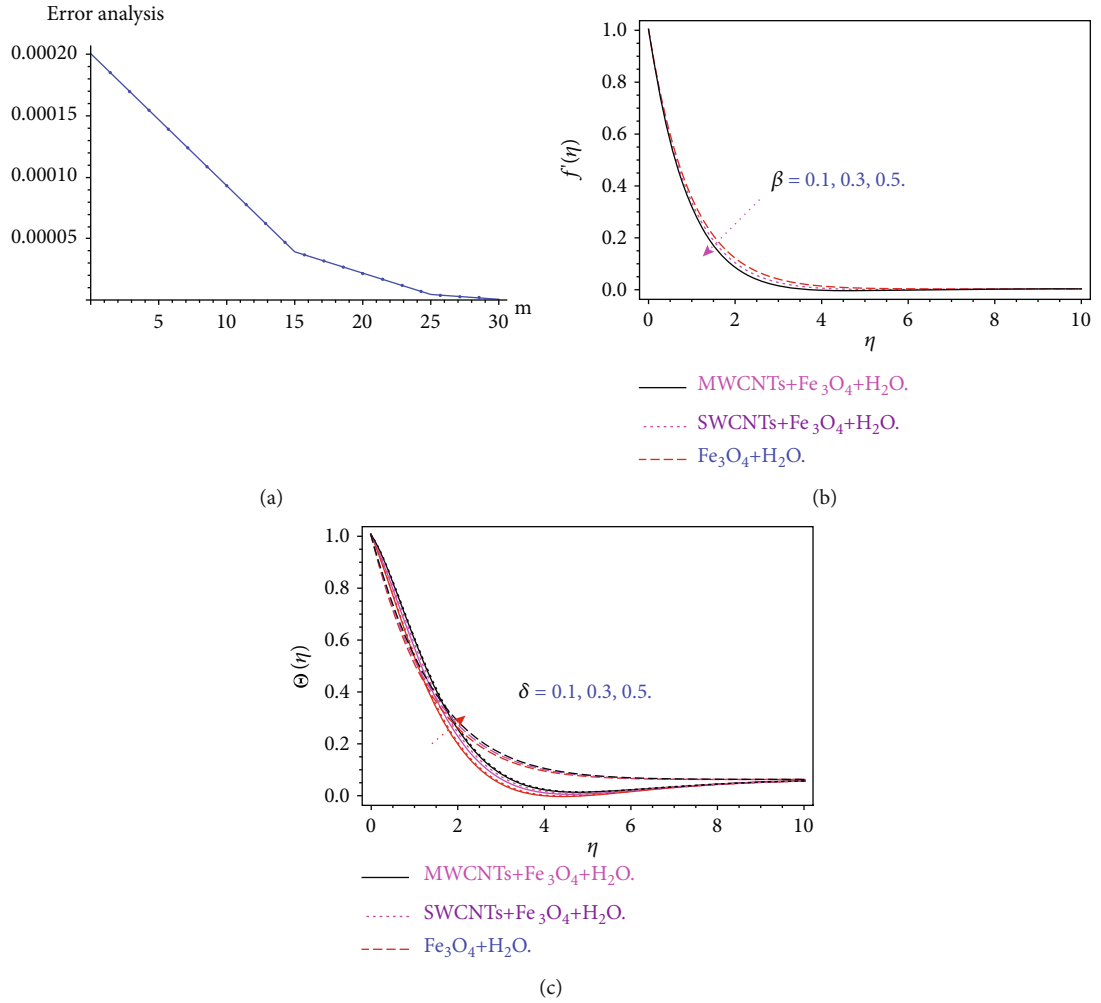

Figure 2: (a)–(c) HAM solution, Casson parameter, and heat absorption\omission parameter influence.

(iii) The non-Newtonian Casson hybrid nanofluid has been used as another extension in the existing literature

(iv) Heat obsorption\omisson has also been considered in the flow regime

(v) This study intends to evaluate and simulate the Darcy-Forchheimer water-based hybrid nanoliquid flow induced by a curved surface that extends

(vi) The second priority is to modify the Saba et al. [48] and Xue [49] model for hybrid nanofluid flow

(vii) The proposed model has been solved by the homotopy analysis method

2. Mathematical Formulation

The Darcy-Forchheimer flow considers CNTs and Fe_3O_4 nanomaterials across an expanding curved sheet. The viscous fluid flow has been expressed in the permeable space by the Darcy-Forchheimer effect. The flow is assumed across the stretching sheet, with radius R, as depicted in Figure 1. The term (r, s) is taken as the space coordinate and (u, v) is the velocity component. Here, $U_w(s) = ae^{s/L}$ is the exponential stretching velocity, T_w is the curved surface, and T_∞ is the ambient temperature. Keeping in view, the above superposition, the energy, and momentum equations along with their boundary conditions are expressed as [9, 36–39, 46]

$$\frac{\partial}{\partial r}((r+R)v) + R\frac{\partial u}{\partial s} = 0, \tag{1}$$

$$\frac{u^2}{r+R} = \frac{1}{\rho_{\text{hnf}}}\frac{\partial p}{\partial r}, \tag{2}$$

$$\begin{aligned} v\frac{\partial u}{\partial r} + \frac{R}{r+R}u\frac{\partial u}{\partial s} + \frac{uv}{r+R} &= -\frac{1}{\rho_{\text{hnf}}}\frac{R}{r+R}\frac{\partial p}{\partial s} \\ &+ \nu_{\text{hnf}}\left(1+\frac{1}{\beta}\right)\left(\frac{\partial^2 u}{\partial r^2} - \frac{u}{(r+R)^2} + \frac{1}{r+R}\frac{\partial u}{\partial r}\right) \\ &- \frac{\nu_{\text{hnf}}}{K^*}u - \frac{1}{\rho_{\text{hnf}}}Fu^2, \end{aligned} \tag{3}$$

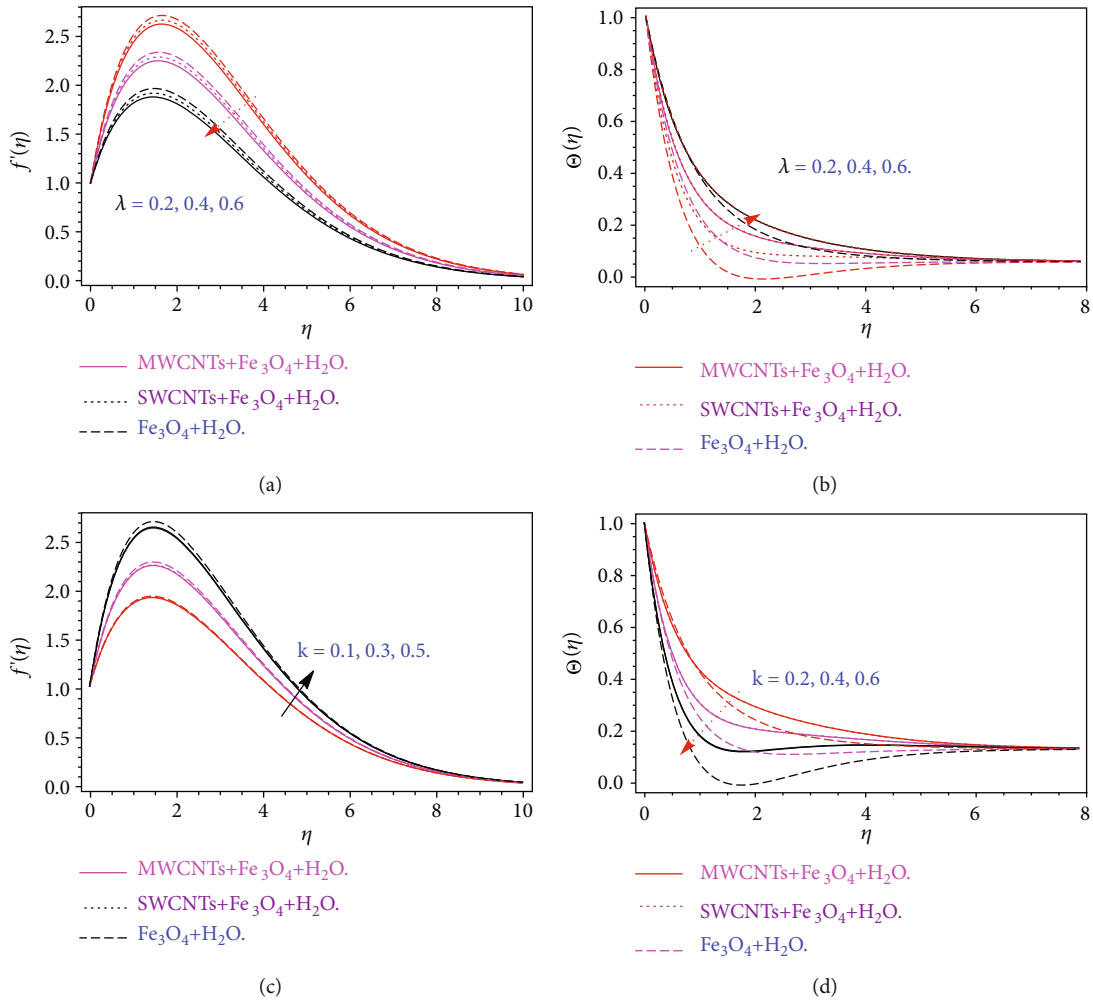

Figure 3: (a, b) Porosity parameter λ impact on the velocity $f'(\eta)$ and temperature profile $\theta(\eta)$. (c, d) Curvature parameter k effect on velocity $f'(\eta)$ and temperature profile, respectively.

$$\left[v\frac{\partial T}{\partial r}+u\frac{\partial T}{\partial s}\frac{R}{r+R}\right]=\alpha_{\text{hnf}}\left(\frac{\partial^2 T}{\partial r^2}+\frac{1}{r+R}\frac{\partial T}{\partial r}\right)+\frac{Q}{(\rho c_p)_{\text{hnf}}}(T-T_\infty), \tag{4}$$

$$\left[v\frac{\partial C}{\partial r}+u\frac{\partial C}{\partial s}\frac{R}{r+R}\right]=D_{\text{hnf}}\left(\frac{\partial^2 C}{\partial r^2}+\frac{1}{r+R}\frac{\partial C}{\partial r}\right). \tag{5}$$

The basic flow conditions are

$$\begin{aligned} v=0,\quad u=U_w(s)=\text{ae}^{s/L},\quad \text{T}=\text{T}_\infty+T_0e^{As/2L}=\text{T}_w,\\ C=C_\infty+C_0e^{As/2L}=C_w,\quad \text{at}\quad r=0,\\ u\longrightarrow 0,\quad \frac{\partial u}{\partial r},\text{T}\longrightarrow T_\infty,\quad C\longrightarrow C_\infty,\quad \text{at}\quad r\longrightarrow\infty. \end{aligned} \tag{6}$$

Here, K^* and $F=C_b/sK^{*1/2}$, are the permeability and inertia factors.

$$\begin{aligned} \upsilon_{\text{hnf}}&=\frac{\mu_{\text{hnf}}}{\rho_{\text{hnf}}},\ \frac{\mu_{\text{hnf}}}{\mu_f}=(1-\phi_1)^{-5/2}(1-\phi_2)^{-5/2},\ \frac{(\rho)_{\text{hnf}}}{(\rho)_f}\\ &=(1-\phi_2)\left\{1-\left(1-\frac{(\rho)\text{Ms}}{(\rho)_f}\right)\phi_1\right\}+\frac{(\rho)_{\text{CNT}}}{(\rho)_f}\phi_2,\\ \frac{k_{\text{hnf}}}{k_{\text{bf}}}&=\left[2\phi_2\frac{k_{CNT}}{(\text{k}_{\text{CNT}}-\text{k}_{\text{bf}})}+(1-\phi_2)-\ln\frac{k_{\text{CNT}}+k_{\text{bf}}}{2\text{k}_{\text{bf}}}\right]\\ &\quad\cdot\left[2\phi_2\frac{k_{\text{bf}}}{(\text{k}_{\text{CNT}}-\text{k}_{\text{bf}})}+(1-\phi_2)-\ln\frac{k_{\text{CNT}}+k_{\text{bf}}}{2\text{k}_{\text{bf}}}\right]^{-1},\\ \frac{k_{\text{bf}}}{k_f}&=\left(k_{\text{MS}}+(\text{m}-1)_{\text{kf}}-\phi_1\left(\text{k}_f-\text{k}_{\text{MS}}\right)\right)^{-1}\\ &\quad\cdot\left(k_{\text{MS}}+(\text{m}-1)_{\text{kf}}-(\text{m}-1)\phi_1\left(\text{k}_f-\text{k}_{\text{MS}}\right),\right.\\ \frac{(\rho\text{C}_p)_{\text{hnf}}}{(\rho\text{C}_p)_f}&=\frac{(\rho C_p)_{\text{CNT}}}{(\rho\text{C}_p)_f}\phi_2+(1-\phi_2)\left\{1-\left(1-\frac{(\rho C_p)\text{Ms}}{(\rho\text{C}_p)_f}\right)\phi_1\right\}. \end{aligned} \tag{7}$$

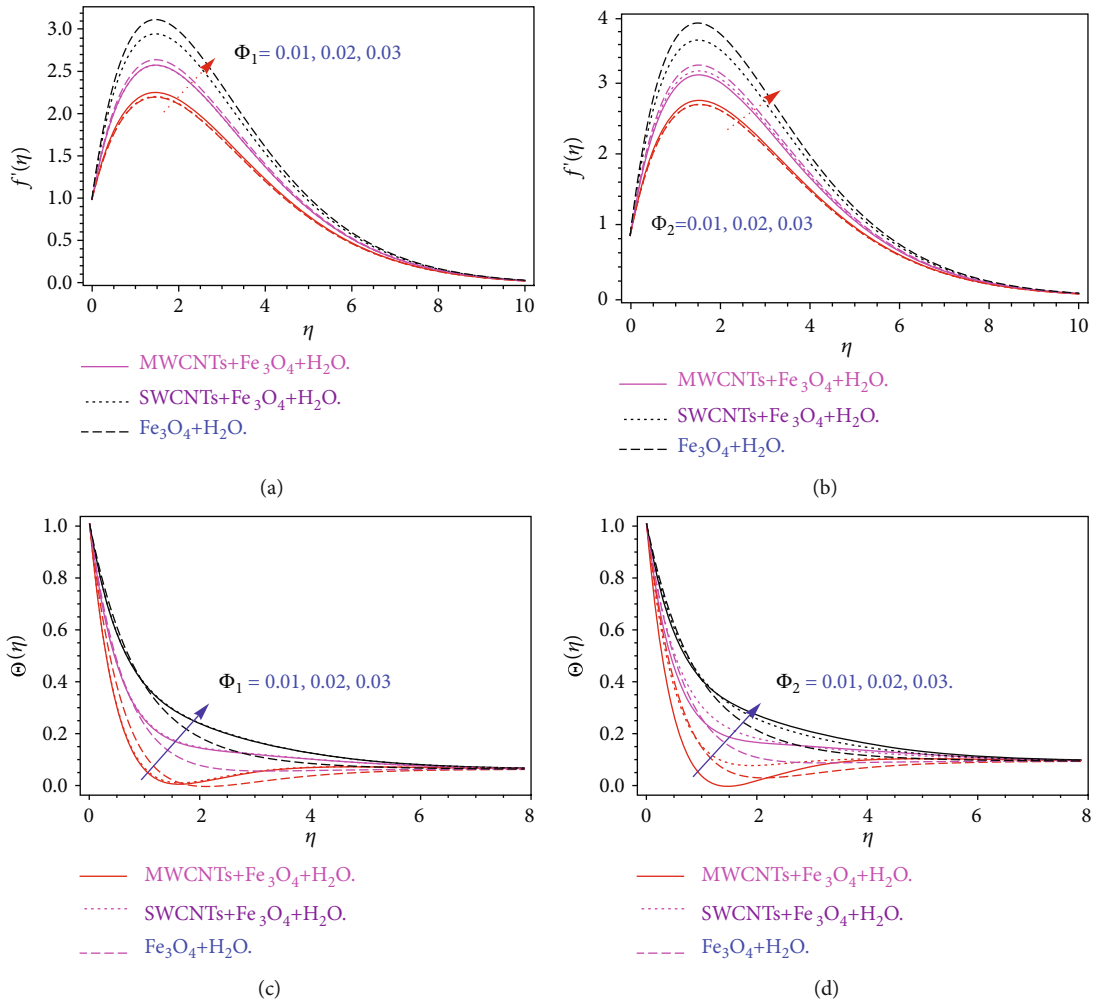

FIGURE 4: (a)–(d) Volume friction parameters ϕ_1 and ϕ_2 impact on the velocity $f'(\eta)$ and temperature profiles $\theta(\eta)$, respectively.

The k_{hnf} is the thermal conductivity, ϕ_1 and ϕ_2 are the volume friction parameters, $(C_p)_{\text{MS}}$ is the specific heat capacity, ρ_{MS} and ρ_{CNT} are specified densities of Fe_3O_4 and CNTs, and Sc is the Schmidt number, respectively.

The transformation variables are [50]

$$\eta = \left(\frac{ae^{s/L}}{2\upsilon_f L}\right)^{1/2} \mathrm{r}, v = -\frac{R}{r+R}\sqrt{\frac{a\upsilon_f e^{s/L}}{2L}}\left(f(\eta)+\eta f'(\eta)\right),$$
$$\mathrm{u} = U_w = ae^{s/L}f'(\eta),$$
$$\mathrm{p} = \rho_f \mathrm{a}^2 \mathrm{e}^{2s/L}\mathrm{H}(\eta), T = T_\infty + T_0 e\frac{As}{2L}\Theta(\eta), C = C_\infty + C_0 e\frac{As}{2L}\Phi(\eta). \tag{8}$$

Thus, by using Eq. (8), Eqs. (2)–(7) yield

$$H' = \left(\frac{(\rho)_{\text{hnf}}}{(\rho)_f}\right)\frac{1}{\eta+K}f'^2, \tag{9}$$

$$\left(1+\frac{1}{\beta}\right)\left(f''' + \frac{1}{\eta+K}f'' - \frac{1}{(\eta+K)^2}f' - 2\lambda f'\right) - (1-\phi_1)^{2.5}(1-\phi_2)^{2.5}\left(\frac{(\rho)_{\text{hnf}}}{(\rho)_f}\right)\left(\frac{\eta+2K}{(\eta+K)^2}K\left(f'\right)^2 - \frac{K}{\eta+K}ff'' - \frac{K}{(\eta+K)^2} + 2Frf'^2\right) = (1-\phi_1)^{2.5}(1-\phi_2)^{2.5}\frac{K}{\eta+K}(4H+\eta H), \tag{10}$$

$$\frac{k_{\text{hnf}}}{k_f}\left(\Theta'' + \frac{1}{\eta+K}\Theta'\right) + \left(\frac{(\rho C_p)_{\text{hnf}}}{(\rho C_p)_f}\right) \cdot \Pr\left[\frac{K}{\eta+K}\left(f\Theta' - Af'\Theta\right) + \delta\Theta\right] = 0, \tag{11}$$

$$(1-\phi_1)(1-\phi_2)\left(\Phi'' + \frac{1}{\eta+K}\Phi'\right) + Sc\left(\frac{K}{\eta+K}f\Phi'\right) = 0. \tag{12}$$

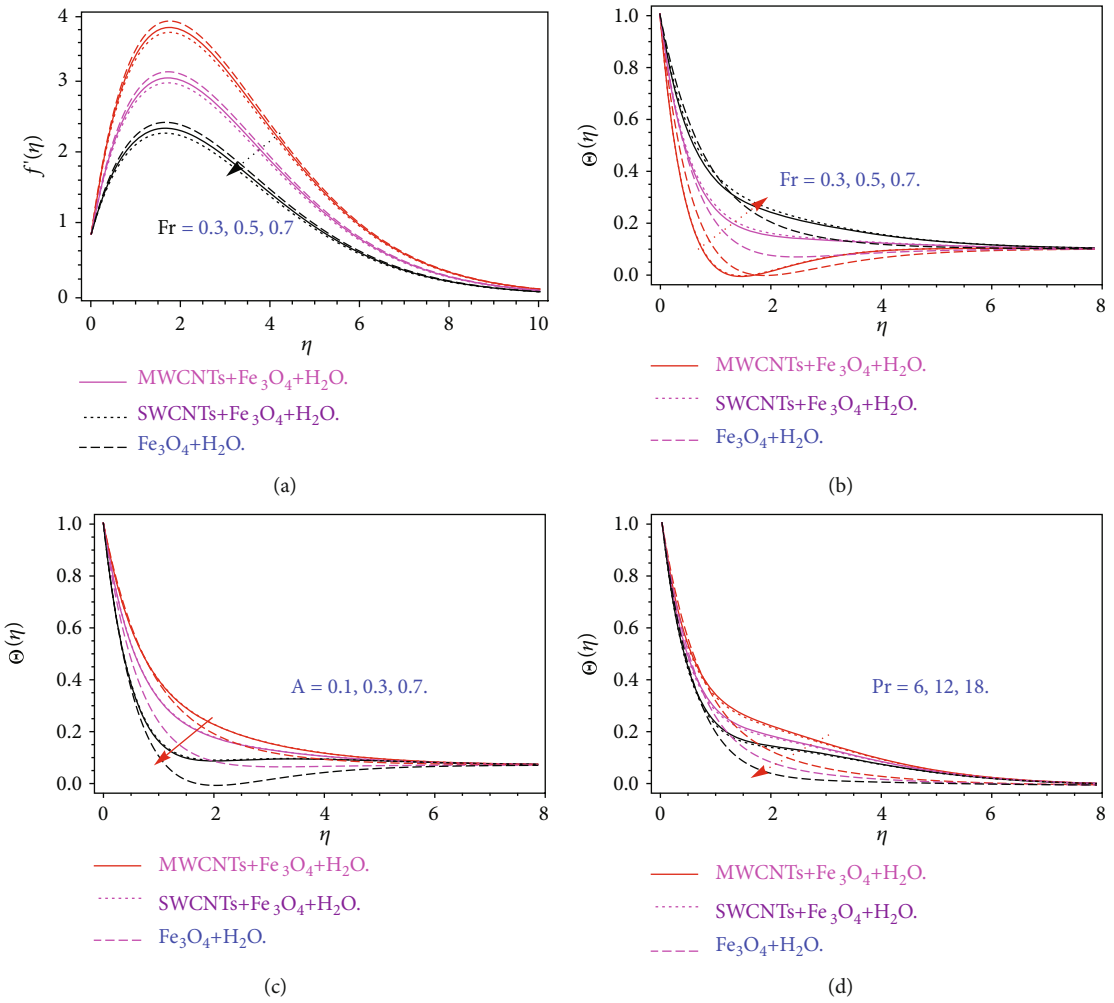

Figure 5: (a, b) Forchheimer parameter Fr impact on the velocity $f'(\eta)$ and temperature profiles $\theta(\eta)$, (c) temperature exponent coefficient, and (d) Prandtl number Pr effects on temperature.

By eliminating H from Eqs. (9) and (10), we get

$$\left(1+\frac{1}{\beta}\right)\left[f'^{v}+\frac{2}{\eta+K}f'''-\frac{1}{(\eta+K)^2}f''+\frac{1}{(\eta+K)^3}\cdot f'-2\lambda\left(f''+\frac{1}{(\eta+K)}f'\right)\right]+\frac{(\rho)_{hnf}}{(\rho)_f}\left[\frac{K}{(\eta+K)^2}ff''+\frac{K}{(\eta+K)}ff'''-\frac{K}{(\eta+K)^3}\cdot ff'\frac{3K}{(\eta+K)^2f'^2}-\frac{3K}{(\eta+K)}\cdot f'f''-2Fr\left(2f'f''+\frac{1}{\eta+K}f'^2\right)\right]=0. \tag{13}$$

The transform conditions are

$$f=0, f'=1, \Phi=1, \Theta=1 \text{at} \eta=0,\quad f'\longrightarrow 0, f''\longrightarrow 0, \Phi\longrightarrow 0, \Theta\longrightarrow 0 \text{at} \eta\longrightarrow\infty, \tag{14}$$

where Fr, λ, and k are the Forchheimer, porosity, and curvature parameters, respectively, which can be rebound as

$$\mathrm{Fr}=\frac{C_b}{K^{*1/2}}, \mathrm{Pr}=\frac{\upsilon_f}{\alpha_f}, \delta=\frac{2\mathrm{QL}}{U_w(\rho c_p)}, k=\left(\frac{ae^{s/L}}{2\upsilon_f L}\right), \lambda=\frac{\upsilon_f L}{K^* U_w}, \mathrm{Sc}=\frac{\upsilon_f}{D_f}. \tag{15}$$

The local Nusselt number, Sherwood Number, and Skin friction are expressed as

$$\frac{L}{S}\left(\frac{\mathrm{Re}}{2}\right)^{\frac{-1}{2}}\mathrm{Nu}_x=-\frac{k_{\mathrm{hnf}}}{k_{bf}}\Theta'(0), \frac{L}{S}\left(\frac{\mathrm{Re}}{2}\right)^{\frac{-1}{2}}Sh_x=-\Phi'(0), \sqrt{\frac{\mathrm{Re}}{2}}C_{fx}=\frac{1}{(1-\phi_1)^{2.5}(1-\phi_2)^{2.5}}\left(1+\frac{1}{\beta}\right)f''(0), \tag{16}$$

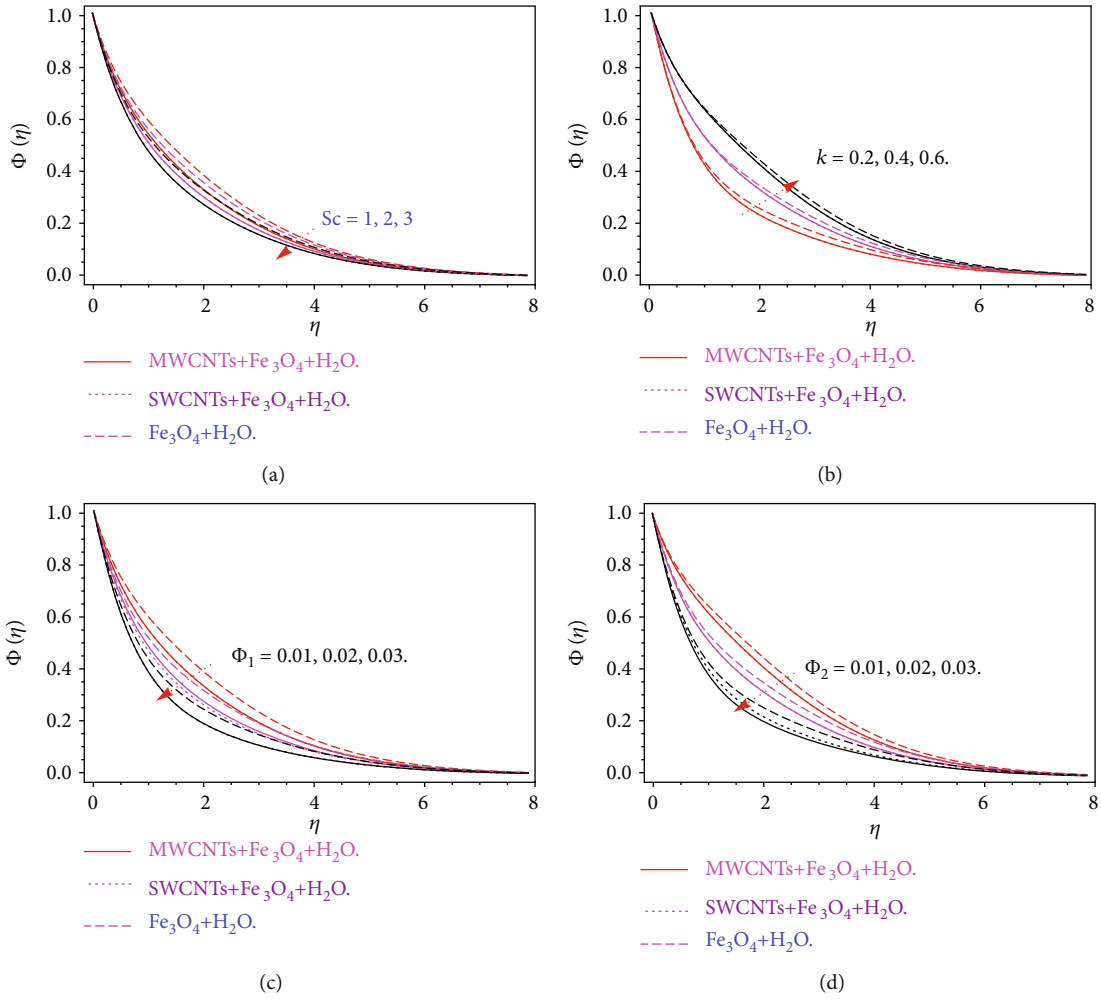

Figure 6: (a) Schmidt number Sc, (b) curvature parameter, and (c, d) volume friction parameters effects on mass transfer profile, respectively.

where local Reynolds number is

$$\mathrm{Re}_x = \frac{u_0 x^2}{\nu l}. \tag{17}$$

3. Problem Solution

For analytical findings, the HAM approach has been utilized to solve the modeled equations, which was firstly introduced by Liao [51–53]. The initial guesses for velocity f_0 and temperature Θ_0 are given as

$$f_0(\eta) = e^{-\eta} - e^{-2\eta}, \Theta_0(\eta) = e^{-\eta}, \Phi_0(\eta) = e^{-\eta}. \tag{18}$$

The linear terms are

$$\mathscr{L}_f(f) = f'^{v} \quad \text{and} \quad \mathscr{L}_\Theta(\Theta) = \Theta''. \tag{19}$$

The expanded form of $\mathscr{L}_f, \mathscr{L}_\Theta$ and $\mathscr{L}_\Phi$ is

$$\begin{aligned} &\mathscr{L}_f\left[\chi_1 + \chi_2\eta + \chi_3\eta^2 + \chi_4\eta^3\right] = 0, \\ &\mathscr{L}_\Theta[\chi_5 + \chi_6\eta] = 0, \mathscr{L}_\Phi[\chi_7 + \chi_8\eta] = 0. \end{aligned} \tag{20}$$

3.1. OHAM Convergence. The converging of the OHAM approach was achieved employing Liao's concept [51–61].

$$\varepsilon_m^f = \frac{1}{l+1}\sum_{j=1}^{l}\left[N_f\left(\sum_{k=1}^{m} f(\eta)\right)_{\eta=j\delta\eta}\right]^2, \tag{21}$$

$$\varepsilon_m^\Theta = \frac{1}{l+1}\sum_{j=1}^{l}\left[N_\Theta\left(\sum_{k=1}^{m} f(\eta), \sum_{k=1}^{m}\Theta(\eta),\right)_{\eta=j\delta\eta}\right]^2, \tag{22}$$

$$\varepsilon_m^\Phi = \frac{1}{l+1}\sum_{j=1}^{l}\left[N_\Phi\left(\sum_{k=1}^{m}\Phi(\eta)\right)_{\eta=j\delta\eta}\right]^2. \tag{23}$$

The sum of residual error is $\varepsilon_m^t = \varepsilon_m^f + \varepsilon_m^\Theta + \varepsilon_m^\Phi$.

4. Results and Discussion

The goal of this portion is forward to see how the temperature and velocity profiles function under the effect of the predicted factors. The flow configuration is shown in Figure 1. The OHAM technique's progress has been

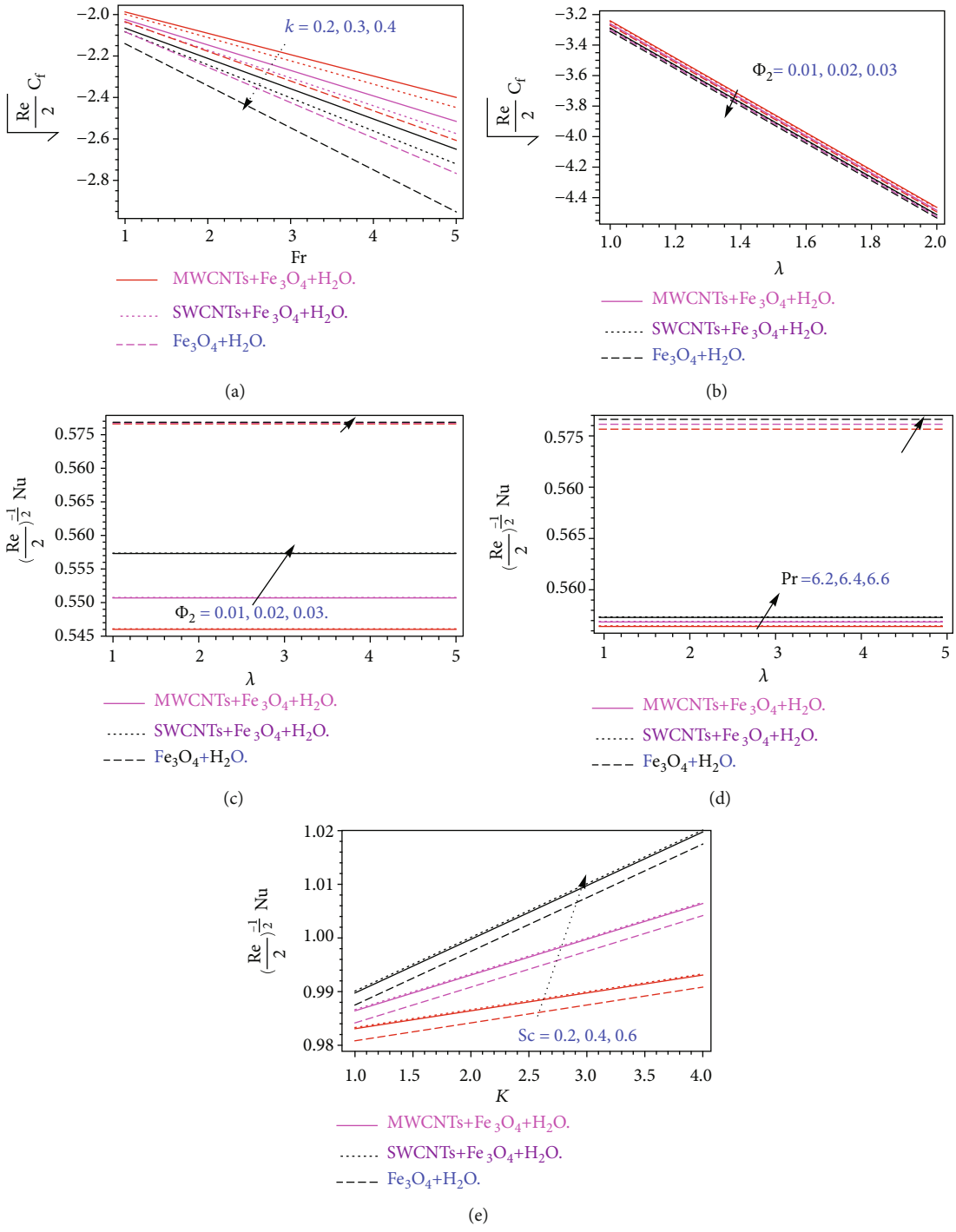

Figure 7: (a) Skin friction $\sqrt{\mathrm{Re}/2}C_{fx}$ for Fr and k, (b) skin friction $\sqrt{\mathrm{Re}/2}C_{fx}$ for λ and ϕ_2, (c) Nusselt number $(L/S)(\mathrm{Re}/2)^{-1/2}Nu_x$ for λ and ϕ_2, (d) Nusselt number $(L/S)(\mathrm{Re}/2)^{-1/2}Nu_x$ for λ and Pr, and (e) Sherwood number $(L/S)(\mathrm{Re}/2)^{-1/2}Sh_x$ for k and Sc.

computed and is depicted in Figure 2(a). Figure 2(b) displays the influence of velocity field versus M. The Lorentz force augments the resistance against the fluid motion and as a result, the velocity reduces with the greater value of the magnetic parameter. The augmentation in the Casson parameter declines the velocity profile. The Casson parameter at the infinity tends to the Newtonian fluid. The larger value of the heat absorption and omission parameter improves the temperature distribution as shown in Figure 2(c). The greater value of the parameter δ improves the temperature distribution. Figure 3 illustrates the effects of the (porosity term) and k on velocity and temperature. This conclusion can be drawn that the velocity $f'(\eta)$ decrease, while the temperature field is increased versus rising values of porosity

Table 1: The numerical properties of nanomaterials and base fluid [27].

	$\rho(\mathrm{kg/m^3})$	C_p(j/kgK)	k(W/mK)
Pure water	997.1	4179	0.613
Fe_3O_4	5200	670	6
SWCNTs	2600	425	6600
MWCNTs	1600	796	300

Table 2: The total residual errors, when $Fr = k = 0.6$, $\phi_1 = 0.02$, $\phi_2 = 0.2$, $\lambda = 0.2$, Pr = 6.3, and $A = 0.4$..

m	ε_m^tSWCNTs	ε_m^tMWCNTs	$\varepsilon_m^t Fe_3O_4$
5	1.8168×10^{-4}	1.9479×10^{-4}	1.4257×10^{-4}
13	1.1223×10^{-5}	1.2354×10^{-5}	1.18312×10^{-5}
23	1.3599×10^{-6}	0.4698×10^{-6}	0.4489×10^{-6}
30	3.2578×10^{-7}	4.3689×10^{-7}	4.1464×10^{-7}

Table 3: The comparative analysis with the published work, when $\phi_1 = \phi_2$, $Fr = k = 0.6$, $\lambda = 0.2$,Pr = 6.3, and $A = 0.4$..

	Hayat et al. [35]	Present
$f''(0)$	0.735	0.7352130
$-\Theta'(0)$	-1.375	-1.3752410
$-\Phi'(0)$	…….	-1.3620189

parameter λ as illustrated in Figures 3(a) and 3(b). Practically, the kinetic viscosity and length of the extending surface are enhanced with the action of the porosity parameter; therefore, such a phenomenon has been observed. On the other hand, the action of curvature parameter k enhances the velocity field and declines the temperature propagation as illustrated in Figures 3(c) and 3(d).

Figures 4(a)–4(d) are sketched to illustrate the consequences of volume friction coefficients ϕ_{CNT} and $\phi_{\mathrm{Fe_3O_4}}$ on velocity and energy propagation. The specific heat capacity of H_2O is greater than much iron and carbon nanoparticles. The addition of nanoparticles in the water reduces its heat-absorbing capacity, which results in an excessive amount of heat in the fluid. These factors cause the enhancement of fluid velocity and thermal energy transition.

Figures 5(a) and 5(b) revealed the influence of Forchhemier number Fr on velocity and temperature profiles, respectively. The increment in the Forchhemier term reduces the fluid velocity and enhances the thermal energy profile. Because the permeability of fluid reduces by the action of the Forchhemier term, therefore, such a phenomenon has been observed. The energy profile declines with the effect of temperature exponent coefficient A and Prandtl number Pr as displayed in Figures 5(c) and 5(d). The thermal diffusivity of fluid rises with the increasing credit of Prandtl number, which results in declination of fluid temperature $\theta(\eta)$ as shown in Figure 5(d). The thickness of the boundary layer improved with the increasing value of Pr and consequently, the temperature profile reduces. Figures 6(a) and 6(b) illustrate to elaborate the consequences of curvature parameter k and Schmidt number Sc on mass transport $\Phi(\eta)$ profile. The mass transition rate reduces with the influence of Schmidt number while enhancing with the positive effects of curvature term, because the fluid mean viscosity becomes thick as the number of carbon and iron oxide particulates continues to increase.

The surface drag force $\sqrt{\mathrm{Re}/2}C_{fx}$ for carbon nanoliquid and Fe_3O_4 is declared via Figures 7(a) and 7(b). It is been evidenced that as the curvature and the volumetric parameters are increased, the skin friction drops. Figures 7(c) and 7(d) demonstrate the numerical results for the Nusselt number $(L/S)(\mathrm{Re}/2)^{-1/2}\mathrm{Nu}_x$. It has been discovered that the heat conversion rate accelerated as the number of carbon nanomaterials in the conventional fluids and the Prandtl number expanded. Figure 7(e) indicates that the Sherwood number $(L/S)(\mathrm{Re}/2)^{-1/2}\mathrm{Sh}_x$ is an enhancing factor of the Schmidt number. Table 1 displays the thermophysical properties of solid substrates and basic fluids. The OHAM technique's consolidation has been computed up to the 30th iteration and is reported in Table 2. Table 3 offers a comparative analysis of the current study to the existing literature.

5. Conclusion

We addressed the Darcy-Forchheimer flow of Casson hybrid nanoliquid induced by an extended curved surface in this problem. The momentum and energy equations are included in the flow model, which is set up as a system of partial differential equations. The "Homotopy analysis method" is used to further build up the analytic arrangement of modeled equations. This mathematical model attempts to highlight the dominance of nanofluid in heat and mass transmission in advanced technologies and industries. The following are the core findings:

(i) The velocity and temperature fields both show positive behaviors against the increasing values of ϕ_1 and ϕ_2 (volume fraction parameters) of CNTs andFe_3O_4

The accumulative values of the Casson parameter decline the hybrid nanofluid motion.

(ii) The employment of CNT and Fe_3O_4 nanomaterials in the base fluid, to regulate the coolant level in industrial equipment, is quite beneficial

(iii) The thermal energy profile shows a reducing trend versus larger values of temperature exponent coefficient A

(iv) High fluid velocity is achieved by increasing the value of k (curvature parameter), while the fluid temperature drops

(v) The temperature and velocity profiles exhibit the opposite tendency when the Forchheimer number

is elevated since the fluid velocity decreases, whereas the temperature profile improves

(vi) The temperature distribution increases for the larger values of the absorption parameter

(vii) The comparison of the recent work with the published work authenticates the obtained results

Data Availability

Data are available in the manuscript.

Conflicts of Interest

No such interest exists.

Acknowledgments

The authors extend their appreciation to the Deanship of Scientific Research at King Khalid University for funding this work through research groups under grant number RGP. 1/260/42.

References

[1] L. J. Crane, "Flow past a stretching plate," *Journal for Applied Mathematics and Physics*, vol. 21, no. 4, pp. 645–647, 1970.

[2] I. A. Hassanien, "Similarity solutions for flow and heat transfer of a viscoelastic fluid over a stretching sheet extruded in a Cross Cooling stream," *ZAMM-Journal of Applied Mathematics and Mechanics/Zeitschrift für Angewandte Mathematik und Mechanik: Applied Mathematics and Mechanics*, vol. 82, no. 6, pp. 409–419, 2002.

[3] T. C. Chiam, "Micropolar fluid flow over a stretching sheet," *ZAMM-Journal of Applied Mathematics and Mechanics/Zeitschrift für Angewandte Mathematik und Mechanik*, vol. 62, no. 10, pp. 565–568, 1982.

[4] P. D. Ariel, "Generalized three-dimensional flow due to a stretching sheet," *ZAMM-Journal of Applied Mathematics and Mechanics/Zeitschrift für Angewandte Mathematik und Mechanik: Applied Mathematics and Mechanics*, vol. 83, no. 12, pp. 844–852, 2003.

[5] K. Bhattacharyya, T. Hayat, and A. Alsaedi, "Exact solution for boundary layer flow of Casson fluid over a permeable stretching/shrinking sheet," *ZAMM-Journal of Applied Mathematics and Mechanics/Zeitschrift für Angewandte Mathematik und Mechanik*, vol. 94, no. 6, pp. 522–528, 2014.

[6] M. Sajid, N. Ali, T. Javed, and Z. Abbas, "Stretching a curved surface in a viscous fluid," *Chinese Physics Letters*, vol. 27, article 024703, 2010.

[7] T. Gul, W. Alghamdi, I. Khan, and I. Ali, "New similarity variable to transform the fluid flow from PDEs into fractional-order ODEs: numerical study," *Physica Scripta*, vol. 96, no. 8, 2021.

[8] M. Imtiaz, T. Hayat, A. Alsaedi, and A. Hobiny, "Homogeneous-heterogeneous reactions in MHD flow due to an unsteady curved stretching surface," *Journal of Molecular Liquids*, vol. 221, pp. 245–253, 2016.

[9] N. C. Rosca and I. Pop, "Unsteady boundary layer flow over a permeable curved stretching/shrinking surface," *European Journal of Mechanics - B/Fluids*, vol. 51, pp. 61–67, 2015.

[10] A. Saeed, W. Alghamdi, S. Mukhtar et al., "Darcy-Forchheimer hybrid nanofluid flow over a stretching curved surface with heat and mass transfer," *PLoS One*, vol. 16, no. 5, article e0249434, 2021.

[11] A. Ali, R. N. Jana, and S. Das, "Radiative CNT-based hybrid magneto-nanoliquid flow over an extending curved surface with slippage and convective heating," *Heat Transfer*, vol. 50, no. 3, pp. 2997–3020, 2021.

[12] K. A. Kumar, V. Sugunamma, and N. Sandeep, "Effect of thermal radiation on MHD Casson fluid flow over an exponentially stretching curved sheet," *Journal of Thermal Analysis and Calorimetry*, vol. 140, no. 5, pp. 2377–2385, 2020.

[13] M. Imtiaz, T. Hayat, and A. Alsaedi, "Convective flow of ferrofluid due to a curved stretching surface with homogeneous-heterogeneous reactions," *Powder Technology.*, vol. 310, pp. 154–162, 2017.

[14] Z. Hussain, S. Muhammad, and M. S. Anwar, "Effects of first-order chemical reaction and melting heat on hybrid nanoliquid flow over a nonlinear stretched curved surface with shape factors," *Advances in Mechanical Engineering*, vol. 13, no. 4, Article ID 168781402199952, 2021.

[15] W. M. Qian, M. I. Khan, F. Shah et al., "Mathematical modeling and MHD flow of micropolar fluid toward an exponential curved surface: heat analysis via ohmic heating and heat source/sink," *Arabian Journal for Science and Engineering*, vol. 2021, pp. 1–12, 2021.

[16] R. U. Haq, Z. H. Khan, and W. A. Khan, "Thermophysical effects of carbon nanotubes on MHD flow over a stretching surface," *Physica E: Low-dimensional Systems and Nanostructures*, vol. 63, pp. 215–222, 2014.

[17] A. Ahmadian, M. Bilal, M. A. Khan, and M. I. Asjad, "Numerical analysis of thermal conductive hybrid nanofluid flow over the surface of a wavy spinning disk," *Scientific Reports*, vol. 10, no. 1, pp. 1–13, 2020.

[18] Y. P. Lv, E. A. Algehyne, M. G. Alshehri et al., "Numerical approach towards gyrotactic microorganisms hybrid nanoliquid flow with the hall current and magnetic field over a spinning disk," *Scientific Reports*, vol. 11, no. 1, pp. 1–13, 2021.

[19] A. Saeed, P. Kumam, T. Gul, W. Alghamdi, W. Kumam, and A. Khan, "Darcy–Forchheimer couple stress hybrid nanofluids flow with variable fluid properties," *Scientific Reports*, vol. 11, no. 1, pp. 1–13, 2021.

[20] T. Gul, A. Qadeer, W. Alghamdi, A. Saeed, S. M. Mukhtar, and M. Jawad, "Irreversibility analysis of the couple stress hybrid nanofluid flow under the effect of electromagnetic field," *International Journal of Numerical Methods for Heat & Fluid Flow*, vol. 2021, 2021.

[21] T. Gul, Z. Ahmed, M. Jawad, A. Saeed, and W. Alghamdi, "Bio-convectional nanofluid flow due to the thermophoresis and gyrotactic microorganism between the gap of a disk and cone," *Brazilian Journal of Physics.*, vol. 51, no. 3, pp. 687–697, 2021.

[22] W. Alghamdi, A. Alsubie, P. Kumam, A. Saeed, and T. Gul, "MHD hybrid nanofluid flow comprising the medication through a blood artery," *Scientific Reports*, vol. 11, no. 1, pp. 1–13, 2021.

[23] Y. X. Li, T. Muhammad, M. Bilal, M. A. Khan, A. Ahmadian, and B. A. Pansera, "Fractional simulation for Darcy-Forchheimer hybrid nanoliquid flow with partial slip over a spinning disk," *Alexandria Engineering Journal*, vol. 60, no. 5, pp. 4787–4796, 2021.

[24] Y. Ding, H. Alias, D. Wen, and R. A. Williams, "Heat transfer of aqueous suspensions of carbon nanotubes (CNT nanofluids)," *International Journal of Heat and Mass Transfer*, vol. 49, no. 1-2, pp. 240–250, 2006.

[25] N. S. Akbar, M. Raza, and R. Ellahi, "Influence of induced magnetic field and heat flux with the suspension of carbon nanotubes for the peristaltic flow in a permeable channel," *Journal of Magnetism and Magnetic Materials*, vol. 381, article 405415, pp. 405–415, 2015.

[26] T. Gul, A. Khan, M. Bilal et al., "Magnetic dipole impact on the hybrid nanofluid flow over an extending surface," *Scientific Reports*, vol. 10, no. 1, pp. 1–13, 2020.

[27] M. Bilal, I. Khan, T. Gul et al., "Darcy-Forchheimer hybrid Nano fluid flow with mixed convection past an inclined cylinder," *CMC-Computers Materials & Continua*, vol. 66, no. 2, pp. 2025–2039, 2021.

[28] S. E. Ahmed, "Effect of fractional derivatives on natural convection in a complex-wavy-wall surrounded enclosure filled with porous media using nanofluids," *ZAMM-Journal of Applied Mathematics and Mechanics/Zeitschrift für Angewandte Mathematik und Mechanik*, vol. 100, no. 1, article e201800323, 2020.

[29] H. Yarmand, S. Gharehkhani, S. F. S. Shirazi et al., "Study of synthesis, stability and thermo-physical properties of graphene nanoplatelet/platinum hybrid nanofluid," *International Communications in Heat and Mass Transfer*, vol. 77, pp. 15–21, 2016.

[30] M. U. Sajid and H. M. Ali, "Thermal conductivity of hybrid nanofluids: a critical review," *International Journal of Heat and Mass Transfer*, vol. 126, pp. 211–234, 2018.

[31] K. G. Kumar, E. H. B. Hani, M. E. H. Assad, M. Rahimi-Gorji, and S. Nadeem, "A novel approach for investigation of heat transfer enhancement with ferromagnetic hybrid nanofluid by considering solar radiation," *Microsystem Technologies*, vol. 27, no. 1, pp. 97–104, 2021.

[32] R. P. Gowda, F. S. Al-Mubaddel, R. N. Kumar et al., "Computational modelling of nanofluid flow over a curved stretching sheet using Koo-Kleinstreuer and Li (KKL) correlation and modified Fourier heat flux model," *Chaos, Solitons & Fractals*, vol. 145, 2021.

[33] R. N. Kumar, R. P. Gowda, A. M. Abusorrah et al., "Impact of magnetic dipole on ferromagnetic hybrid nanofluid flow over a stretching cylinder," *Physica Scripta*, vol. 96, no. 4, article 045215, 2021.

[34] A. Zeeshan, Z. Ali, M. R. Gorji, F. Hussain, and S. Nadeem, "Flow analysis of biconvective heat and mass transfer of two-dimensional couple stress fluid over a paraboloid of revolution," *International Journal of Modern Physics B*, vol. 34, no. 11, p. 2050110, 2020.

[35] K. M. Sanni, S. Asghar, M. Jalil, and N. F. Okechi, "Flow of viscous fluid along a nonlinearly stretching curved surface," *Results in Physics*, vol. 7, pp. 1–4, 2017.

[36] M. Jawad, A. Saeed, T. Gul, and A. Khan, "The magnetohydrodynamic flow of a nanofluid over a curved exponentially stretching surface," *Heat Transfer*, vol. 50, no. 6, pp. 5356–5379, 2021.

[37] A. Saeed, P. Kumam, S. Nasir, T. Gul, and W. Kumam, "Nonlinear convective flow of the thin film nanofluid over an inclined stretching surface," *Scientific Reports*, vol. 11, no. 1, pp. 1–15, 2021.

[38] T. Hayat, M. Rashid, M. Imtiaz, and A. Alsaedi, "MHD convective flow due to a curved surface with thermal radiation and chemical reaction," *Journal of Molecular Liquids*, vol. 225, p. 482, 2017.

[39] T. Hayat, R. Sajjad, R. Ellahi, A. Alsaedi, and T. Muhammad, "Homogeneous-heterogeneous reactions in MHD flow of micropolar fluid by a curved stretching surface," *Journal of Molecular Liquids*, vol. 240, p. 209, 2017.

[40] N. F. Okechi, M. Jalil, and S. Asghar, "Flow of viscous fluid along an exponentially stretching curved surface," *Results in Physics*, vol. 7, pp. 2851–2854, 2017.

[41] Z. Asghar, N. Ali, R. Ahmed, M. Waqas, and W. A. Khan, "A mathematical framework for peristaltic flow analysis of non-Newtonian Sisko fluid in an undulating porous curved channel with heat and mass transfer effects," *Computer Methods and Programs in Biomedicine*, vol. 182, 2019.

[42] T. Hayat, R. S. Saif, R. Ellahi, T. Muhammad, and B. Ahmad, "Numerical study for Darcy-Forchheimer flow due to a curved stretching surface with Cattaneo-Christov heat flux and homogeneous-heterogeneous reactions," *Results in Physics*, vol. 7, pp. 2886–2892, 2017.

[43] Z. Abbas, M. Naveed, and M. Sajid, "Hydromagnetic slip flow of nanofluid over a curved stretching surface with heat generation and thermal radiation," *Journal of Molecular Liquids*, vol. 215, pp. 756–762, 2016.

[44] Z. Mehmood, Z. Iqbal, E. Azhar, and E. N. Maraj, "Nanofluidic transport over a curved surface with viscous dissipation and convective mass flux," *Zeitschrift für Naturforschung A*, vol. 72, no. 3, pp. 223–229, 2017.

[45] N. Acharya, "Active-passive controls of liquid di-hydrogen mono-oxide based nanofluidic transport over a bended surface," *International Journal of Hydrogen Energy*, vol. 44, no. 50, pp. 27600–27614, 2019.

[46] P. Forchheimer, "Water movement through ground," *Journal of the Association of German Engineers.*, vol. 45, pp. 1782–1788, 1901.

[47] M. Muskat, "The flow of homogeneous fluids through porous media," *Soil Science.*, vol. 46, no. 2, p. 169, 1938.

[48] F. Saba, N. Ahmed, U. Khan, and S. T. Mohyud-Din, "A novel coupling of (CNT-Fe3O4/H2O) hybrid nanofluid for improvements in heat transfer for flow in an asymmetric channel with dilating/squeezing walls," *International Journal of Heat and Mass Transfer*, vol. 136, pp. 186–195, 2019.

[49] Q. Z. Xue, "Model for thermal conductivity of carbon nanotube-based composites," *Physica B: Condensed Matter.*, vol. 368, pp. 302–307, 2005.

[50] T. Hayat, F. Haider, T. Muhammad, and A. Alsaedi, "Numerical treatment for Darcy-Forchheimer flow of carbon nanotubes due to an exponentially stretching curved surface," *Journal of Central South University.*, vol. 26, no. 4, pp. 865–872, 2019.

[51] T. Hayat, F. Haider, T. Muhammad, and A. Alsaedi, "Numerical study for Darcy-Forchheimer flow of nanofluid due to an exponentially stretching curved surface," *Results in Physics.*, vol. 8, pp. 764–771, 2018.

[52] S. J. Liao, "An optimal homotopy-analysis approach for strongly nonlinear differential equations," *Communications in Nonlinear Science and Numerical Simulation*, vol. 15, no. 8, pp. 2003–2016, 2010.

[53] S. J. Liao, Ed., *Advances in the Homotopy Analysis Method, Chapter 7*, World Scientific Press, 2013.

[54] T. Gul and K. Ferdous, "The experimental study to examine the stable dispersion of the graphene nanoparticles and to look

at the GO–H2O nanofluid flow between two rotating disks," *Nano*, vol. 8, no. 7, pp. 1711–1727, 2018.

[55] M. Jawad, A. Saeed, T. Gul, and A. Bariq, "MHD Darcy-Forchheimer flow of Casson nanofluid due to a rotating disk with thermal radiation and Arrhenius activation energy," *Journal of Physics Communications.*, vol. 5, no. 2, article 025008, 2021.

[56] A. Rehman, Z. Salleh, and T. Gul, "Heat transfer of thin film flow over an unsteady stretching sheet with dynamic viscosity," *Journal of Advanced Research in Fluid Mechanics and Thermal Sciences*, vol. 81, no. 2, pp. 67–81, 2021.

[57] M. Jawad, A. Saeed, T. Gul, Z. Shah, and P. Kumam, "Unsteady thermal Maxwell power law nanofluid flow subject to forced thermal Marangoni convection," *Scientific Reports*, vol. 11, no. 1, pp. 1–14, 2021.

[58] A. Khan, W. Kumam, I. Khan et al., "Chemically reactive nanofluid flow past a thin moving needle with viscous dissipation, magnetic effects and hall current," *PLoS One*, vol. 16, no. 4, article e0249264, 2021.

[59] A. Khan, A. Saeed, A. Tassaddiq et al., "Bio-convective micropolar nanofluid flow over thin moving needle subject to Arrhenius activation energy, viscous dissipation and binary chemical reaction," *Case Studies in Thermal Engineering.*, vol. 25, 2021.

[60] M. Bilal, T. Gul, A. Alsubie, and I. Ali, "Axisymmetric hybrid nanofluid flow with heat and mass transfer amongst the two gyrating plates," *Zeitschrift für Angewandte Mathematik und Mechanik*, vol. 101, no. 11, 2021.

[61] L. Ali, A. Tassaddiq, R. Ali et al., "A new analytical approach for the research of thin-film flow of magneto hydrodynamic fluid in the presence of thermal conductivity and variable viscosity," *ZAMM-Journal of Applied Mathematics and Mechanics/Zeitschrift für Angewandte Mathematik und Mechanik*, vol. 101, no. 2, 2021.